Understanding the Interactions of Climate and Land Use Changes with Runoff Components in Spatial-Temporal Dimensions in the Upper Chi Basin, Thailand

Rattana Hormwichian , Siwa Kaewplang , Anongrit Kangrang , Jirawat Supakosol , Kowit Boonrawd , Krit Sriworamat , Sompinit Muangthong , Songphol Songsaengrit , Haris Prasanchum *

Posted Date: 5 September 2023

doi: 10.20944/preprints202309.0338.v1

Keywords: climate change; land use change; QSWAT; runoff components; Upper Chi Basin

Article

Understanding the Interactions of Climate and Land Use Changes with Runoff Components in Spatial-Temporal Dimensions in the Upper Chi Basin, Thailand

Rattana Hormwichian [1], Siwa Kaewplang [1], Anongrit Kangrang [1], Jirawat Supakosol [2], Kowit Boonrawd [2], Krit Sriworamat [3], Sompinit Muangthong [4], Songphol Songsaengrit [5] and Haris Prasanchum [5,*]

[1] Faculty of Engineering, Mahasarakham University, Mahasarakham, Thailand; rattana.h@msu.ac.th (R.H); siwa.k@msu.ac.th (S.K); anongrit.k@msu.ac.th (A.K)
[2] Faculty of Industry and Technology, Rajamangala University of Technology Isan, Sakon Nakhon Campus, Sakon Nakhon, Thailand; jirawat.ko@rmuti.ac.th (J.K); kowit.bo@rmuti.ac.th (K.B)
[3] Faculty of Engineering, Ubonratchathani University, Ubonratchathani, Thailand; kritubu@gmail.com (K.S)
[4] Faculty of Engineering and Technology, Rajamangala University of Technology Isan, Nakhon Ratchasima, Thailand; sompinit.mu@rmuti.ac.th (S.M)
[5] Faculty of Engineering, Rajamangala University of Technology Isan, Khon Kaen Campus, Khon Kaen, Thailand; songphol.so@rmuti.ac.th (S.S); haris.pr@rmuti.ac.th (H.P)
* Correspondence: haris.pr@rmuti.ac.th

Abstract: Climate and land use changes are major factors affecting runoff in regional basins. Understanding variation by considering interactions among hydrological components is an important process for water resource management. This study aimed to assess the variation of future runoff in the Upper Chi Basin, Northeastern Thailand. QSWAT hydrological model was integrated to 3 CMIP6 GCMs including ACCESS-CM2, MIROC6, and MPI-ESM1-2-LR under SSP245 and SSP585 scenarios during 2023 – 2100. Land Change Modeler (LCM) was also used for future land use simulation. The results revealed that future average of long-term precipitation and temperature tended to increase while forest land tended to decrease and be replaced by sugarcane plantations. The accuracy assessment of baseline year runoff calculation by QSWAT during 1997 – 2022 showed acceptable result as can be seen from R^2, NSE, RSR, and PBIAS indices. This result could lead to temporal and spatial simulation of future runoff. Likewise, runoff of 2 SSPs scenarios tended to increase consecutively, especially in SSP585 scenario. In addition, in case of long-term spatial changes in the subbasins scale, over 90% of the area, from upstream to outlet point, tended to get higher due to 2 major factors including future increased precipitation and changes in cultivation, which would be influential to groundwater and interflow components respectively. Methodology and result of this study can be useful to stakeholders in understanding changes in hydrological system so that they can apply it to develop a strategy for water resource management and handling factors affecting different dimensions properly and sustainably.

Keywords: climate change; land use change; QSWAT; runoff components; Upper Chi Basin

1. Introduction

Climate change has been affecting our world for over a decade, especially more physical effects of natural disasters on environment and socio-economic aspects. Although there have been attempts to prevent any loss, damage or destruction in all related dimensions, climate change is considered as the top prioritized concern about causes of natural disasters, such as extreme drought [1] and monsoon flood [2]. In addition, factors of variation affecting hydrologic system are changes of land use and land cover (LULC) in a river basin [3] caused by human activities, such as agriculture,

 doi:10.20944/preprints202309.0338.v1

industry, habitation, transportation, and socio-economic factors [4–6], which lead to higher water consumption [7].

Climate and land use changes have a huge amount of influence on the ecosystem of water resource [8], and they are variable differently in each area. When both mentioned influential factors are revoked rapidly, they can be a cause of runoff change in terms of its quantity and process as well as a cause of water flow behavior and related components [9]. Generally, processes of understanding, analysis, and evaluation reflect long-term spatial and temporal evolution of outcomes that show water balance components, including surface runoff, groundwater flow, infiltration, evapotranspiration, soil moisture, etc [10,11]. The processes are to simplify situation explanation of changes by time and to categorize runoff components according to hydrologic system used as basic data for making decisions on water resource management or used as a communication tool in an organization effectively to understand stakeholders involved in river basin management [12]. For this reason, understanding quantitative, qualitative, and social effects of variation of climate and land use changes on water resource is now selected as a main topic of study throughout the world [13].

To understand these effects, Hydrological Model has been used for analysis and evaluation because it is capable of prediction with high reliability, and it has been recognized as a decision support system in developing river basin plans [14]. Applying Hydrological Model to General Circulation Models (GCMs) and prediction of LULC has been the most popular approaches for analyzing and understanding problems over the past decade. Semi-distributed Hydrological Model has been widely used all over the world because it uses spatial data associated with meteorological and hydrological conditions, divides basin sizes and scopes according to physical characteristics, analyzes sensitivity of related hydrological variables, and gives reliable results and reasonable explanation. One of the most widely used models in the world is Soil and Water Assessment Tool (SWAT) [15], which connects to ArcGIS model for its operation [16].

Currently, engineers and hydrologists can access a model and develop a simpler way to use it. Many researches have applied open-source software to model development. Dile et al. [17] developed a QSWAT model, which was a new version of open-source interface merging QGIS [18] with SWAT, as a tool for hydrological analysis [19–21]. Similar to data preparation for future weather forecast, data can be currently collected from many available sources publicized by different institutes all over the world without charge, especially GCMs in the Coupled Model Intercomparison Project (CMIP), such as Earth System Grid Federation (ESGF) [22]. However, before using data from GCMs, both downscaling and bias correction are needed in order to gain accurate data consistent with regional basin area. In simulating future land use changes, several models have been recently developed to meet the needs of spatial change studies and to be in line with current advancement of geo-information technology. Related studies have used Land Change Modeler (LCM) [23] because of its ability to analyze and predict the future of land use changes [24] and urban growth [25].

The Upper Chi Basin (UCB) locate in Northeastern Thailand was selected for this study because it is the main headwaters forest of the region. One major problem found in this area was ecosystem changes affected by community growth and economic activities that leaded to higher needs of freshwater use. Forest resource degradation was considered as one of the major problems because soil erosion caused by deforestation was found. Moreover, the headwaters were sloping and woody, so flash flood could strike community area in case of deforestation. Meanwhile water reservoir and flood defense system were insufficient, and people tried to deforest by changing some of the land into plantation and habitation. From this situation, it leaded to the changes in surface runoff and shallow river, which were inefficient in flood control.

The main objective of this research was to assess the effects of climate and land use changes on runoff in the UCB. The research applied QSWAT model and used future climate data of 3 GCMs from CMIP6 including ACCESS-CM2, MIROC6, and MPI-ESM1-2-LR under SSP245 and SSP585 scenarios. The LCM model was used for future land use simulation. In reporting research results and discussion, focuses on climate and land use change, efficiency of Hydrological Model, and relationships among runoff components. The studied was divided into 4 future period subbasins between 2023 – 2100; (1) 2023 – 2040, (2) 2041 – 2060, (3) 2061 – 2080, and (4) 2081 – 2100, in order to

Preprints (www.preprints.org) | NOT PEER-REVIEWED | Posted: 5 September 2023 doi:10.20944/preprints202309.0338.v1

demonstrate spatial and temporal changes and compare to the baseline (BL) year 2000-2022. Methodology and results of this research were expected to be used as a guideline for understanding current and future hydrological changes. Moreover, the study results are useful that agencies use for decision making on water resource management planning and all stakeholders plan their ways to deal with any dimensions of possible effects appropriately and sustainably.

2. Materials and Methods

2.1. Study Area

The UCB is located in the northeastern region of Thailand and is one of the Chi subbasins. The Chi River is a main regional river with 3,287 km^2 catchment area. The main river flows from the western upland, where it includes mountain ridge covered with dense forest, downward to the eastern exit as presented in Figure 1. Its average annual precipitation is 1,221.9 mm and average annual temperature is 28.1 °C. Average monthly maximum temperature is 36.3 °C in April and minimum temperature is 18.0 °C in December. Its average annual relative humidity is 69.0%. Average monthly maximum relative humidity is 94.0% in September and minimum relative humidity is 35.0% in March.

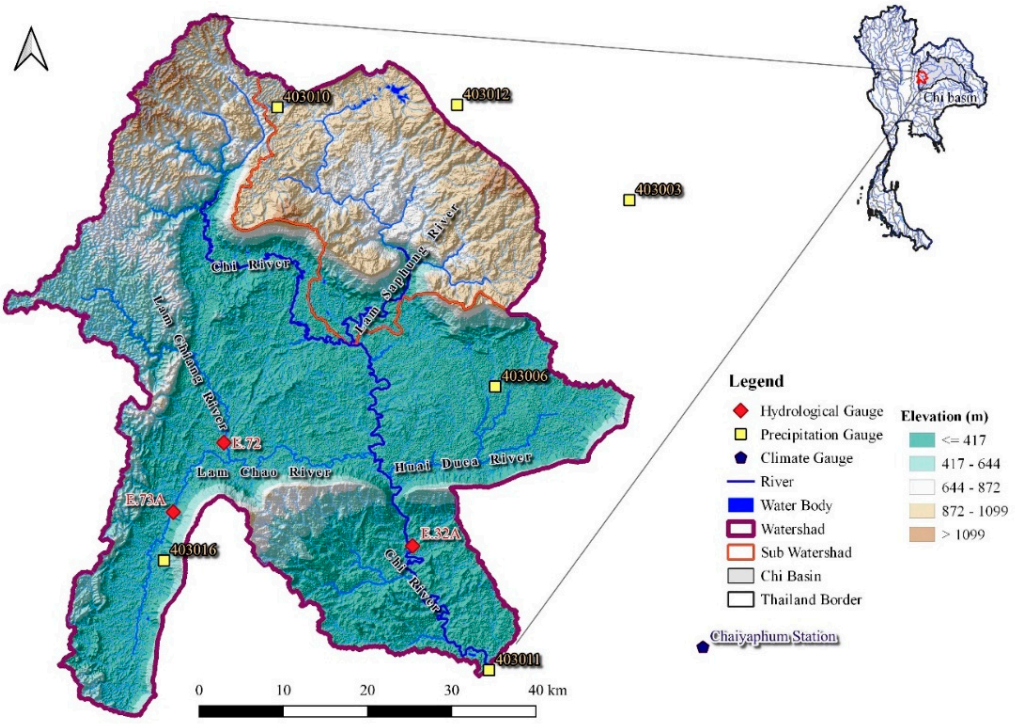

Figure 1. Topography of the UCB.

2.2. Data Collection

The data collected for this study consisted of two types: 1) meteorological and hydrological data, and 2) physical data of basin including daily precipitation from 6 stations, daily maximum and minimum temperatures from 1 station between 1997 - 2022 from the Thailand Meteorological Department, and recorded runoff at Station E.32A, E72, and E.73A between 1997 - 2022 from the Royal Irrigation Department as shown in Figure 1. Physical data of the basin included 30x30 m Digital Elevation Model (DEM) from the Shuttle Radar Topography Mission (SRTM), land use map, and soil map from the Land Development Department as presented in Table 1 and Figure 2.

 doi:10.20944/preprints202309.0338.v1

Table 1. Data used in the study.

Data Type	Resolution	Year	Source
Digital Elevation Model (DEM)	30x30 m	2017	SRTM (Earth Resources Observation and Science (EROS) Center, 2017)
Land use map	30x30 m	2019	Land Development Department (LDD)
Soil series	30x30 m	2018	Land Development Department (LDD)
Precipitation, minimum-maximum temperatures, relative humidity, wind speed, and sunshine hour	daily	1997 - 2022	Thailand Meteorological Department (TMD)
Recorded runoff at observed stations: E.32A, E72 and E.73A	monthly	1997 - 2022	Royal Irrigation Department (RID)

2.3. Global Climate Model and Bias Correction

2.3.1. Global Climate Model (GCM)

In analyzing future climate change, future changes in precipitation and maximum and minimum temperature data are considered. These data are used for future analysis of changes in precipitation using QSWAT model. Analyzing future climate change starts from using climate data in 3 CMIP6 GCMs including ACCESS-CM2, MIROC6, and MPI-ESM1-2-LR to analyze the changes in precipitation and maximum and minimum temperature. In case of future scenarios, Shared Socioeconomic Pathways (SSP) for SSP245 and SSP585 was considered, where SSP245 was a future pathway having moderate radiation forcing and updating RCP4.5, and SSP585 was a future pathway having high radiation forcing used to study effects, adaptation and relief as well as updating RCP8.5. For RCP8.5, it was regarded as the worst case because it was predicted that greenhouse gas emissions might be high. In Table 2, it shows GCM with 4 periods of time of future climate change; 1) 2023 – 2040, 2) 2041 – 2060, 3) 2061 – 2080, and 4) 2081 – 2100.

Table 2. 3 CMIP6 GCMs for future climate analysis.

Models	Resolution (km)	Institutes	References
ACCESS-CM2	250x250	Commonwealth Scientific and Industrial Research Organization, Australia	[26]
MIROC6	250x250	Model for Interdisciplinary Research on Climate, Japan	[27]
MPI-ESM1-2-LR	250x250	Max Planck Institute for Meteorology, Germany	[28]

2.3.1. Data Bias Correction

Bias correction of GCMs in this study used the Climate Model data for hydrologic modeling (CMhyd) and Linear scaling (LS) to gain the representatives of the UCB. Climate data including precipitation as well as maximum and minimum temperature during 1997-2002 were inputted for monthly factor calculation. Climate data during 1997 – 2015 were corrected for all models to get close to the values previously inputted into CMhyd model by linear scaling [29]. Bias correction by CMhyd was globally applied to different models in many studies [30–32].

Preprints (www.preprints.org) | NOT PEER-REVIEWED | Posted: 5 September 2023 doi:10.20944/preprints202309.0338.v1

2.4. Land Use Change Scenarios

This study analyzed future changes in land use using the Land Change Modeler (LCM), which is a sub program of a software system called TerrSet developed by Clark Labs, Clark University, USA [33]. This model analyzed a tendency of land use change based on land use data from 2 periods of time; 2015 and 2019 (Figure 2) to gain temporal correlations. Then LMC analyzed transition potential of possible land use and cover according to variables related to future changes using Multi-Layer Perceptron (MLP), which created potential maps of changes [34].

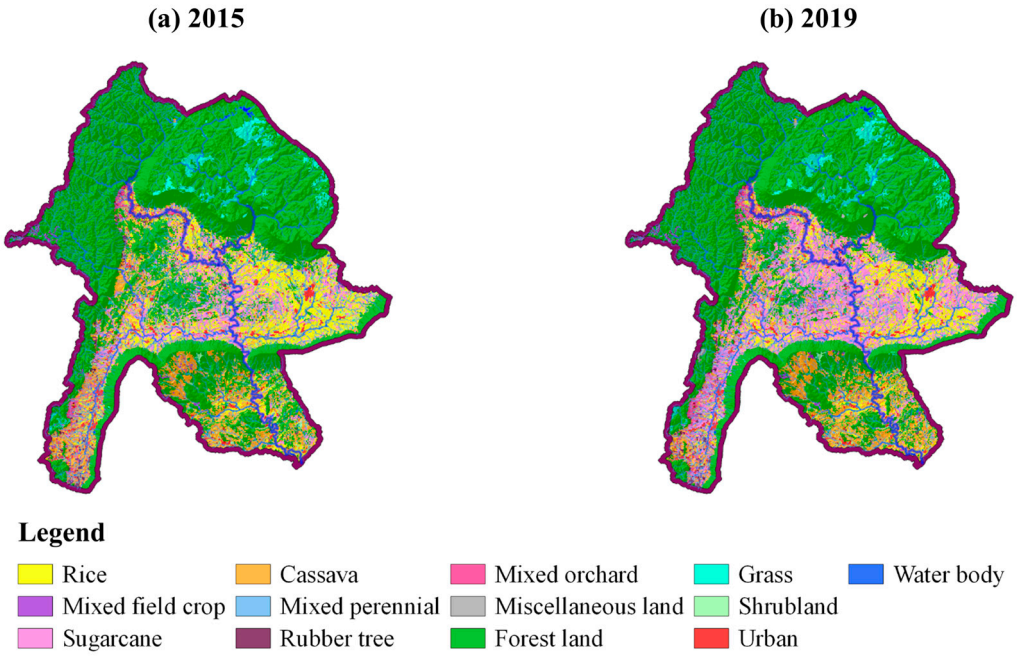

Figure 2. Land use map in BL year; (a) 2015, (b) 2019.

2.5. Runoff Analysis by QSWAT Model

2.5.1. QSWAT Model

QSWAT is a hydrological model that can simulate physical basins by distributing the parameters according to the physical conditions of the actual area. It is also able to predict the effects of climate change and land use on runoff, sediment, and agricultural chemicals [35–40]. In addition, its calculation process is so reliable and is widely used not only in Thailand but also around the world [41]. The QSWAT works together with geographic information systems (GISs) including ArcGIS (or ArcSWAT), ArcView (or AVSWAT), and QGIS (or QSWAT). This study employed QSWAT from QGIS, which can be downloaded free of charge. QSWAT helped divide the basin into different subbasins. Within each subbasin, it was split into "Hydrologic Response Units (HRUs)" that were developed from data of overlaid Digital Elevation Model (DEM), land use, and soil group by modeling a hydrological cycle using QSWAT model and a water balance as the below equation (Equation 1):

$$SW_t = SW_o + \sum_{i=1}^{t} (R_{day} - Q_{surf} - E_a - w_{seep} - Q_{qw}) \quad (1)$$

where SW_t is soil water content at time or t (mm), SW_0 is initial soil water content (mm), R_{day} is cumulative precipitation on day i (mm), Q_{surf} is cumulative runoff on day i (mm), E_a is evapotranspiration on day i (mm), w_{seep} is percolation on day i (mm), Q_{gw} is underground water amount on day i (mm) [42].

Preprints (www.preprints.org) | NOT PEER-REVIEWED | Posted: 5 September 2023 doi:10.20944/preprints202309.0338.v1

2.5.2. Delimitation of subbasin and input data

Subbasins in the QSWAT were delimitated using data in Digital Elevation Model (DEM) with existing natural watercourse data. This study used 30x30 m DEM, and there were 31 sub basins divided by QSWAT model. Then HRUs were identified relying on physical data, 13 type land use, 11 type soil data, and 3 level slope (0-5%, 5-10%, and >10%). These were overlaid each other to gain 670 HRUs. Finally, daily 26-year climate data (1997 – 2022) were inputted; (1) precipitation data obtained from 6 measuring stations and (2) climate data obtained from 1 weather station including maximum and minimum temperature, relative humidity, wind speed, and sunshine duration.

2.5.3. Sensitivity analysis of parameters

Parameters in QSWAT of this study were analyzed their sensitivity by SWAT-CUP [43,44] using Sequential Uncertainty Fitting version 2 (SUFI2) [45] for parameters affecting runoff at observed stations; E.32A E.72 and E.73A, and it was monthly 26-year analysis (1997 – 2022). There were 300 duplicates carried out to analyze sensitivity of 14 parameters using Nash-Sutcliffe Efficiency (NSE) as Objective Function. The Global Sensitivity Analysis result obtained from SWAT-CUP showed t-Stat and P-Value. Both of them were from hypothesis testing of parameters that was related to the Objective Function.

2.5.4. Calibration and Model Validation

Similar to sensitivity analysis of parameters, a technique SUFI2 was employed for calibration by SWAT-CUP to compare data between runoff in QSWAT and monthly 14-year runoff recorded in 3 stations (E.32A, E.72, and E.73A) between 1997 – 2010. There were 300 duplicates conducted, and Nash-Sutcliffe Efficiency (NSE) was defined as the Objective Function. After gaining optimal values, they were inputted into QSWAT to calculate R^2, NSE, RSR, and PBIAS (Equations 2 - 5) for each station. Also, the model was validated for its reliability based on monthly 11-year validation (2011 – 2022):

$$R^2 = \left[\frac{\sum_{i=1}^{n}(O_i - \bar{O})(P_i - \bar{P})}{\sqrt{\sum_{i=1}^{n}(O_i - \bar{O})^2}\sqrt{\sum_{i=1}^{n}(P_i - \bar{P})^2}}\right] \quad (2)$$

$$NSE = \frac{\sum_{i=1}^{n}(O_i - \bar{O})^2 - \sum_{i=1}^{n}(P_i - \bar{P})^2}{\sum_{i=1}^{n}(O_i - \bar{O})^2} \quad (3)$$

$$RSR = \left[\frac{\sum_{i=1}^{n}(O_i - P_i)^2}{\sqrt{\sum_{i=1}^{n}(O_i - \bar{O})^2}}\right] \quad (4)$$

$$PBIAS = \left[\frac{\sum_{i=1}^{n}(O_i - P_i) \times 100}{\sum_{i=1}^{n}(O_i)}\right] \quad (5)$$

where O_i is recorded runoff from observed station, $\bar{O}$ is average recorded runoff from observed station, P_i is runoff calculated by model, $\bar{P}$ is average runoff calculated by model, and i is data order.

2.6. Evaluation of Future Changes in Runoff Components

Future climate data with completed bias collection collected from 3 types of GCM under SSP245 and SSP585 scenarios consisted of precipitation and maximum and minimum temperatures data during 2023 – 2100. Prepared data of future land use by LCM consisted of 4 datasets including 2040, 2060, 2080, and 2100. These data were entered into a reliable QSWAT that was calibrated and validated in terms of runoff calculation during 1997 – 2022 BL year by statistical evaluation of 4

Preprints (www.preprints.org) | NOT PEER-REVIEWED | Posted: 5 September 2023 doi:10.20944/preprints202309.0338.v1

indices. Therefore, QSWAT was expected to calculate future runoff under climate and land use change situations. Then runoff components were evaluated and presented the changes pattern in both spatial and temporal forms in the form of graphs and spatial maps respectively.

3. Results and Discussion

3.1. Climate Change Scenarios

3.1.1. Precipitation

According to the analysis of future monthly average precipitation of the UCB obtained from 3 GCMs compared with 2000 – 2022 BL year, the result was in line as shown in Figure 3. Future monthly precipitation of SSP245 scenario was slightly higher than BL year. In SSP585 scenario from May to October 2061 – 2100, the precipitation would be higher, especially in August (300 – 350 mm). For initial prediction during 2023 - 2060, it showed value close to BL year. According to annual precipitation calculation, 2000 – 2022 showed an average precipitation of 1,221.9 mm per year. When comparing with the result from ACCESS-CM2 model, precipitation was decreased by 1.8 – 3.4% for SSP245 scenario and 11.3 – 14.6% for SSP585 scenario. MIROC-6 and MPI-ESM1-2-LR models showed 2.3 – 9.9% and 10.1 – 21.8% respectively higher annual average precipitation. Both SSP245 and SSP585 scenarios also had their 2.2 – 14.9% and 10.7 – 53.6% respectively higher value. Figure 4 show temporal changes in annual average precipitation in the long future.

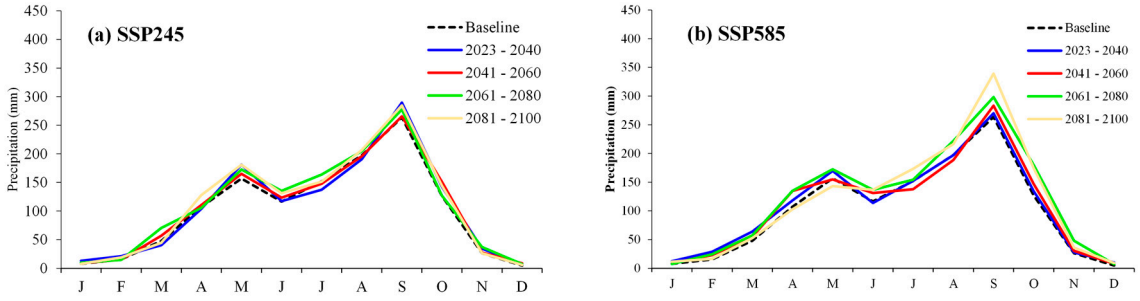

Figure 3. Future average precipitation from 3 GCMs; (a) SSP245, (b) SSP585.

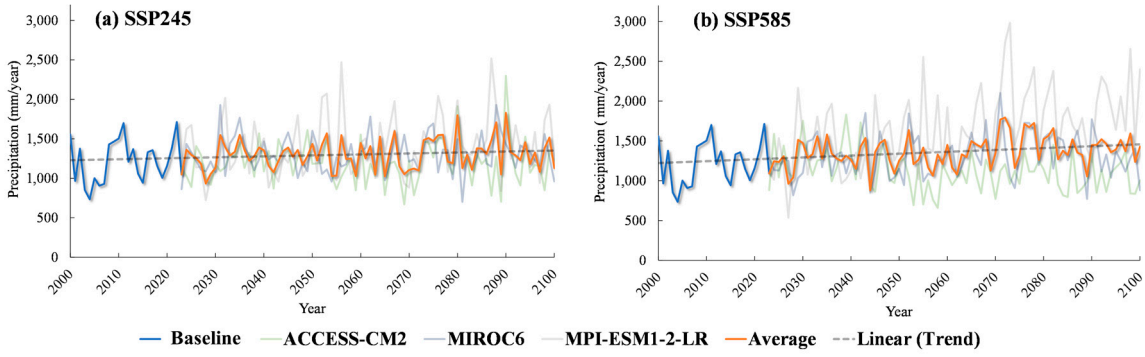

Figure 4. Annual precipitation tendencies; (a) SSP245, (b) SSP585.

3.1.2. Maximum and minimum temperatures

After gaining monthly average from maximum and minimum temperatures analysis of 3 GCMs as shown in Figure 5, both scenarios showed their average close to BL year during initial predicted year (2023 - 2040). The SSP245 scenario during 2041 – 2100 showed slightly different average, or its value increased future time periods. On the other hand, SSP585 scenario showed its trend higher than BL year. Its average of maximum and minimum temperatures during 2081 – 2100 was 40.3 °C in April while the average of BL year in the same month was 36.5 °C or increased by 10.4%. According to Figure 6, the annual maximum and minimum temperatures during 2000 – 2022 was 33.1 °C and 23.1

Preprints (www.preprints.org) | NOT PEER-REVIEWED | Posted: 5 September 2023 doi:10.20944/preprints202309.0338.v1

°C respectively. When comparing to each model, SSP585 scenario was higher than SSP245 scenario. The ACCESS-CM2 model displayed average maximum of 35.4 °C that was 6.9% higher than BL year average, increased from 0.5 °C to 3.8 °C between 2023 – 2100 in SSP585 scenario. In case of average minimum temperature, the SSP245 scenario increased from 0.6 to 2.1 °C while the SSP585 scenario increased from 0.6 to 4.1 °C. The ACCESS-CM2 model displayed average maximum of 25.6 °C that was 10.8% higher than BL year average. Both scenarios indicated that their average maximum temperature of 26.8 °C that was 16.0% higher than BL year average. When considering overall long-term changes in maximum and minimum temperatures, both predicted scenarios tended to be higher in temperature.

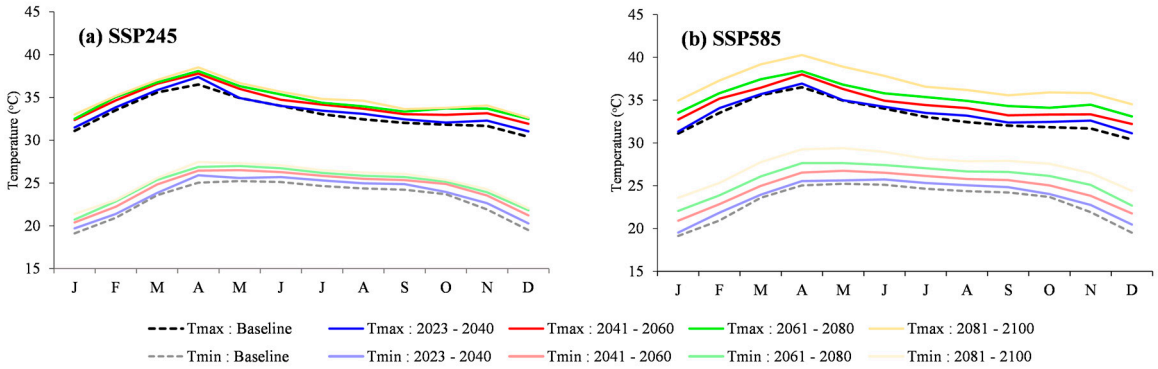

Figure 5. Future monthly average temperature of 3 GCMs; (a) SSP245, (b) SSP585.

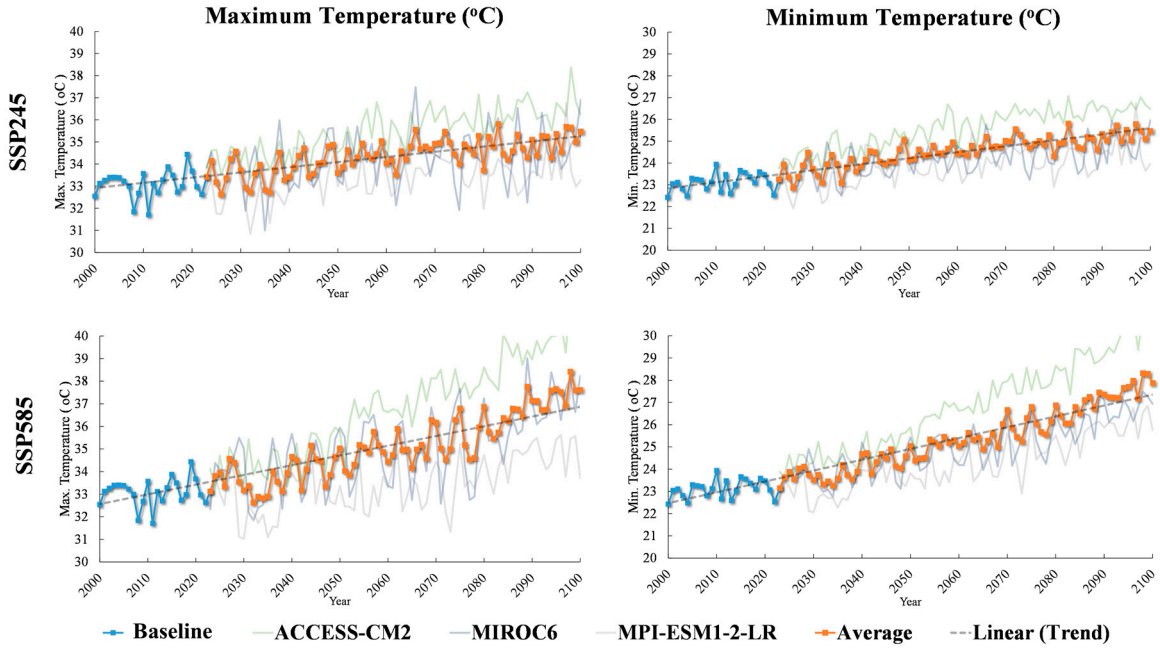

Figure 6. Trends of average annual maximum and minimum temperatures.

3.2. Land Use Change

To analyze the future land use change in the UCB, there were 4 future time periods predicted (2040, 2060, 2080, and 2100) to be in line with climate change analysis. The results of the study of land use changes during the base year compared with the simulation in the future obtained from LCM can be shown in Table 3. While Figure 7 presents the simulation results of spatial change patterns in the future, divided into 4 time periods compared to the BL years (2015 and 2019). For the analysis of the study results, it is divided into 2 parts as follows;

Preprints (www.preprints.org) | NOT PEER-REVIEWED | Posted: 5 September 2023 doi:10.20944/preprints202309.0338.v1

3.2.1. Future decrease in area

Forest was the most abundant land in the UCB. It had 1,886.4 km² or 57.4% of total area (3,287.6 km²). The simulation result of future land use changes reflected that forest land tended to get highest decrease in area. It would decrease to 1,595.9 km² in 2040 (decreased by 290.5 km² or 15.4% from 2019) and tends to decrease until 2100 to 1,238 km² (decreased by 648.4 km² or 34.3% from 2019). Rice field showed the second highest decrease in area. Its area was 313.9 km² in 2019. According to simulation result of future area in 2040, the decrease in variable trend would be 149.7 km². However, the area was predicted to slightly increase between 167.4 and 183.4 km² during 2060 – 2100. Cassava plantation showed the third highest decrease in area. Its area was 254.3 km² in 2019. According to simulation result, it was predicted to decrease during 2040 – 2060, or the area would be 120.2 km² and 119.9 km² respectively. However, it would slightly increase during 2080 – 2100 or 123.9 km² – 126.8 km² respectively. In terms of decrease in area of forest (green), rice field (yellow), and cassava plantation (orange), they were considered from spatial distribution. Likewise, the LMC showed future prediction result that reflected that central and southern basin areas were particularly replaced by cassava plantation.

3.2.2. Future increase in area

The result of future land use simulation revealed that sugarcane plantation would be significantly expanded. According to the result analysis of changes in sugarcane plantation during 2015 – 2019 BL year, it was expanded from 256.8 km² up to 483.2 km². According to future change simulation by LCM, sugarcane plantation would be expanded 1,022.2 – 1,328.6 km² or 111.6 – 175% during 2040 – 2100. According to the spatial expansion, future expanded sugarcane plantation would take the place of forest and rice field that could be obviously seen during the day and in southern basin area. Another type of land use that would tend to increase after the sugarcane was mixed field crop. Its increase would change from 28.9 km² to 65.1 km² in 2100 while rubber tree and mixed orchard lands demonstrated their slightly future increase and decrease between 31.9% – 33.3% and 24.8% – 30.1% respectively.

Table 3. Future land use change compared to BL year (2019).

Land use types	BL		Future periods							
			2040		2060		2080		2100	
	2015	2019	A (km²)	Diff. 2019 (%)	A (km²)	Diff. 2019 (%)	A (km²)	Diff. 2019 (%)	A (km²)	Diff. 2019 (%)
Rice	412.1	313.9	149.7	-52.3	167.4	-46.7	177.9	-43.3	183.4	-41.6
Mixed field crop	18.2	28.9	51.9	79.6	59.1	104.4	62.9	117.4	65.1	125.3
Sugarcane	256.8	483.2	1,022.2	111.6	1,173.9	143.0	1,268.0	162.4	1,328.6	175.0
Cassava	289.7	254.3	120.2	-52.7	119.9	-52.9	123.9	-51.3	126.8	-50.1
Mixed perennial	16.2	17.8	17.8	0.0	17.8	0.0	17.8	0.0	17.8	0.0
Rubber tree	31.1	38.1	50.2	31.9	51.3	34.7	51.1	34.1	50.8	33.3
Mixed orchard	39.2	48.3	62.9	30.1	61.7	27.6	60.8	25.7	60.3	24.8
Miscellaneous land	6.6	11.4	13.5	18.7	12.1	6.5	11.7	3.2	11.6	2.4
Forest land	1,998.1	1,886.4	1,595.9	-15.4	1,419.9	-24.7	1,308.6	-30.6	1,238.0	-34.4

Preprints (www.preprints.org) | NOT PEER-REVIEWED | Posted: 5 September 2023 doi:10.20944/preprints202309.0338.v1

Grass	87.0	78.4	76.2	-2.7	77.6	-0.9	78.0	-0.5	78.1	-0.4
Shrubland	38.1	29.4	29.4	0.0	29.4	0.0	29.4	0.0	29.4	0.0
Urban	56.8	58.7	58.7	0.0	58.7	0.0	58.7	0.0	58.7	0.0
Water body	37.7	38.7	38.7	0.0	38.7	0.0	38.7	0.0	38.7	0.0
Total area	**3,287.4**	**3,287.4**	**3,287.4**		**3,287.4**		**3,287.4**		**3,287.4**	

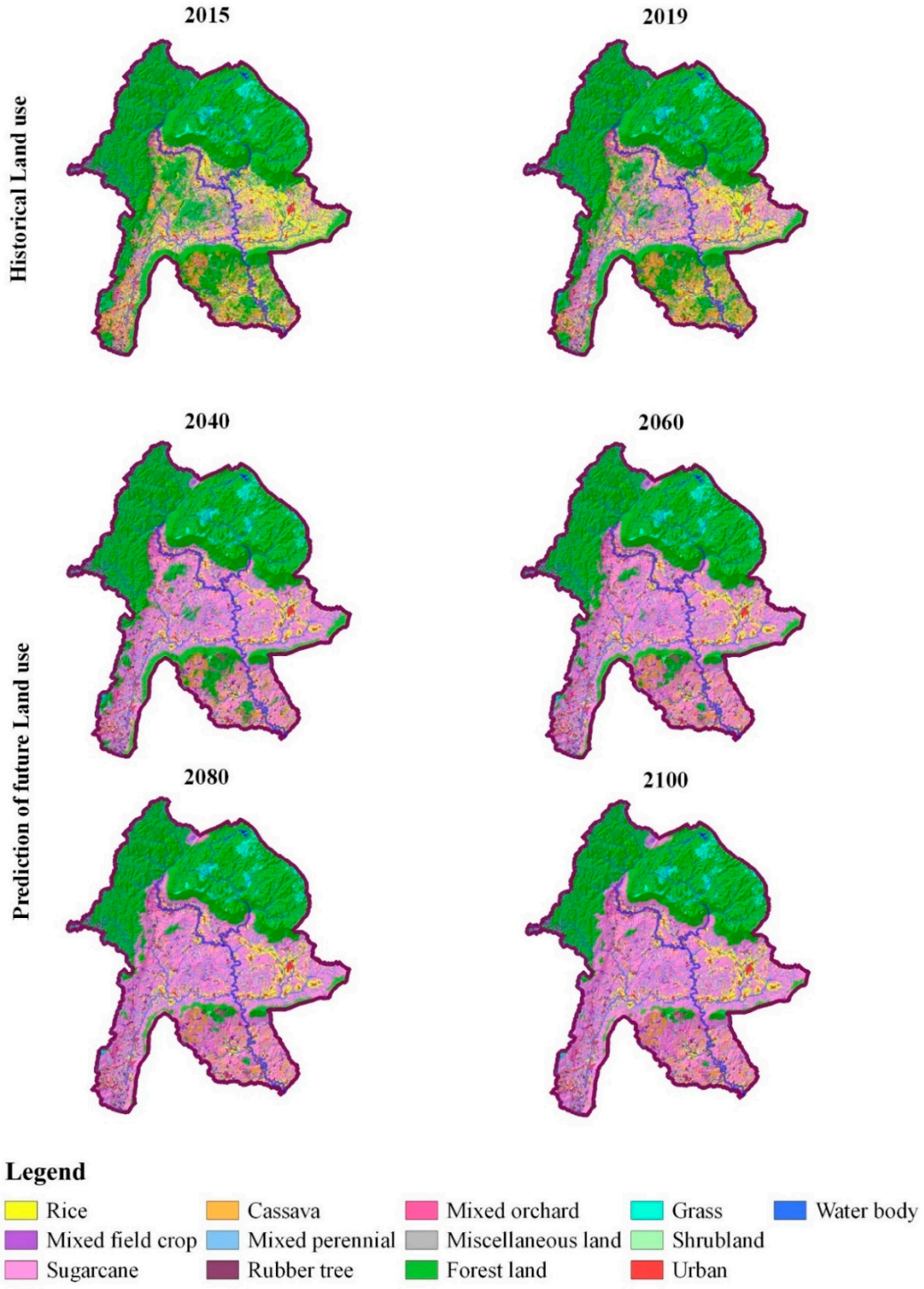

Figure 7. Future land use in the UCB resulted from Land Change Modeler (LCM).

Preprints (www.preprints.org) | NOT PEER-REVIEWED | Posted: 5 September 2023 doi:10.20944/preprints202309.0338.v1

3.3. Efficiency Evaluation of QSWAT

3.3.1. Sensitivity Analysis of Parameters

The result of sensitivity analysis by SWAT-CUP presented t-Stat and P-Value, which were obtained from hypothesis testing of parameters that were related to Objective Function. The result of Global Sensitivity Analysis is presented in Table 4. It revealed that the first 3 most influential parameters to the changes in runoff were CN2, SOL_AWC, and GWQMN by considering t-Stat with highest negative or positive value (regardless of symbols) and by considering P-Value that was lowest or close to zero, which meant that the parameter was very significantly sensitive to Objective Function [46]. Other parameters and suitable parameters for runoff calculation also illutrated in Table 4.

Table 4. Parameters for sensitivity analysis and model calibration. .

Rank	Parameter	Description	Fitted Value	Adjust Range	t-Stat	P-value
1	R_CN2.mgt	SCS runoff curve number	-0.01	-0.1 – 0.3	-12.44	0.0000
2	R_SOL_AWC.sol	Available water capacity of the soil layer	0.21	-0.1 – 0.3	4.31	0.0000
3	V_GWQMN.gw	Threshold depth of water in the shallow aquifer required for return flow to occur (mm)	1258.33	0 – 5000	4.02	0.0001
4	V_CH_N1.sub	Manning's "n" value for the tributary channels	0.076	0.01 – 0.1	1.96	0.0507
5	V_GW_DELAY.gw	Groundwater delay (days)	180.50	30 – 450	-1.78	0.0769
6	V_CH_N2.rte	Manning's "n" value for the main channel	0.037	0.01 – 0.1	-1.16	0.2463
7	V_CH_K2.rte	Effective hydraulic conductivity in main channel alluvium	97.67	0 – 200	-1.03	0.3033
8	V_EPCO.bsn	Plant uptake compensation factor	0.69	0 – 1	-0.87	0.3865
9	R_SLSUBBSN.hru	Average slope length	-0.12	-0.2 – 0.2	0.46	0.6487
10	V_ALPHA_BF.gw	Baseflow alpha factor (days)	0.24	0 – 1	-0.45	0.6500
11	R_SOL_K.sol	Saturated hydraulic conductivity	-0.08	-0.1 – 0.2	0.39	0.7001
12	V_REVAPMN.gw	Threshold depth of water in the shallow aquifer for "revap" to occur (mm)	124.17	0 – 500	-0.16	0.8745

Preprints (www.preprints.org) | NOT PEER-REVIEWED | Posted: 5 September 2023 doi:10.20944/preprints202309.0338.v1

Rank	Parameter	Description	Fitted Value	Adjust Range	t-Stat	P-value
13	V_ESCO.bsn	Soil evaporation compensation factor	0.89	0.1 − 0.2	-0.14	0.8896
14	V_GW_REVAP.gw	Groundwater "revap" coefficient	0.15	0 − 1	0.01	0.9937

3.3.2. Model calibration and validation

Sensitivity analysis by SWAT-CUP could give optimal parameters for the UCB. These parameters were used for correcting parameter in QSWAT and calculating R^2, NSE, RSR, and PBIAS of Station E.32A, E.72, and E.73A. The correlation in statistics between monthly 14-years calibration (1997 – 2010) and monthly 12-years validation (2011 – 2022) can be summarized in Table 5 and Figure 12. According to the Table, values of R^2, NSE, RSR, and PBIAS were acceptable and standardized [47] based on the criteria for monthly runoff evaluation as shown in Table 6.

Table 5. Correlation in statistics of runoff by model calibration and validation.

Stations	Model stage	Evaluation statistics			
		R^2	NSE	RSR	PBIAS
E.32A	Calibration (1997-2010)	0.79	0.67	0.58	30.19
	Validation (2011-2022)	0.89	0.78	0.47	13.23
	Overall (1997-2022)	0.84	0.73	0.52	22.76
E.72	Calibration (1997-2010)	0.67	0.53	0.68	15.95
	Validation (2011-2022)	0.73	0.70	0.54	-0.53
	Overall (1997-2022)	0.70	0.64	0.60	8.18
E.73A	Calibration (1997-2010)	0.75	0.69	0.56	30.45
	Validation (2011-2022)	0.76	0.71	0.54	-9.89
	Overall (1997-2022)	0.73	0.70	0.55	13.15

Table 6. Performance ratings for evaluation metrics for a monthly time step.

Performance Rating	R^2	NSE	RSR	PBIAS
Very Good	$0.75 < R^2 \leq 1.00$	$0.75 < NSE \leq 1.00$	$0.00 < RSR \leq 0.50$	$PBIAS < \pm 10$
Good	$0.65 < R^2 \leq 0.75$	$0.65 < NSE \leq 0.75$	$0.50 < RSR \leq 0.60$	$\pm 10 \leq PBIAS < \pm 15$
Satisfactory	$0.50 < R^2 \leq 0.65$	$0.50 < NSE \leq 0.65$	$0.60 < RSR \leq 0.70$	$\pm 15 \leq PBIAS < \pm 25$
Unsatisfactory	$R^2 \leq 0.50$	$NSE \leq 0.50$	$RSR > 0.70$	$PBIAS \geq \pm 25$

Preprints (www.preprints.org) | NOT PEER-REVIEWED | Posted: 5 September 2023 doi:10.20944/preprints202309.0338.v1

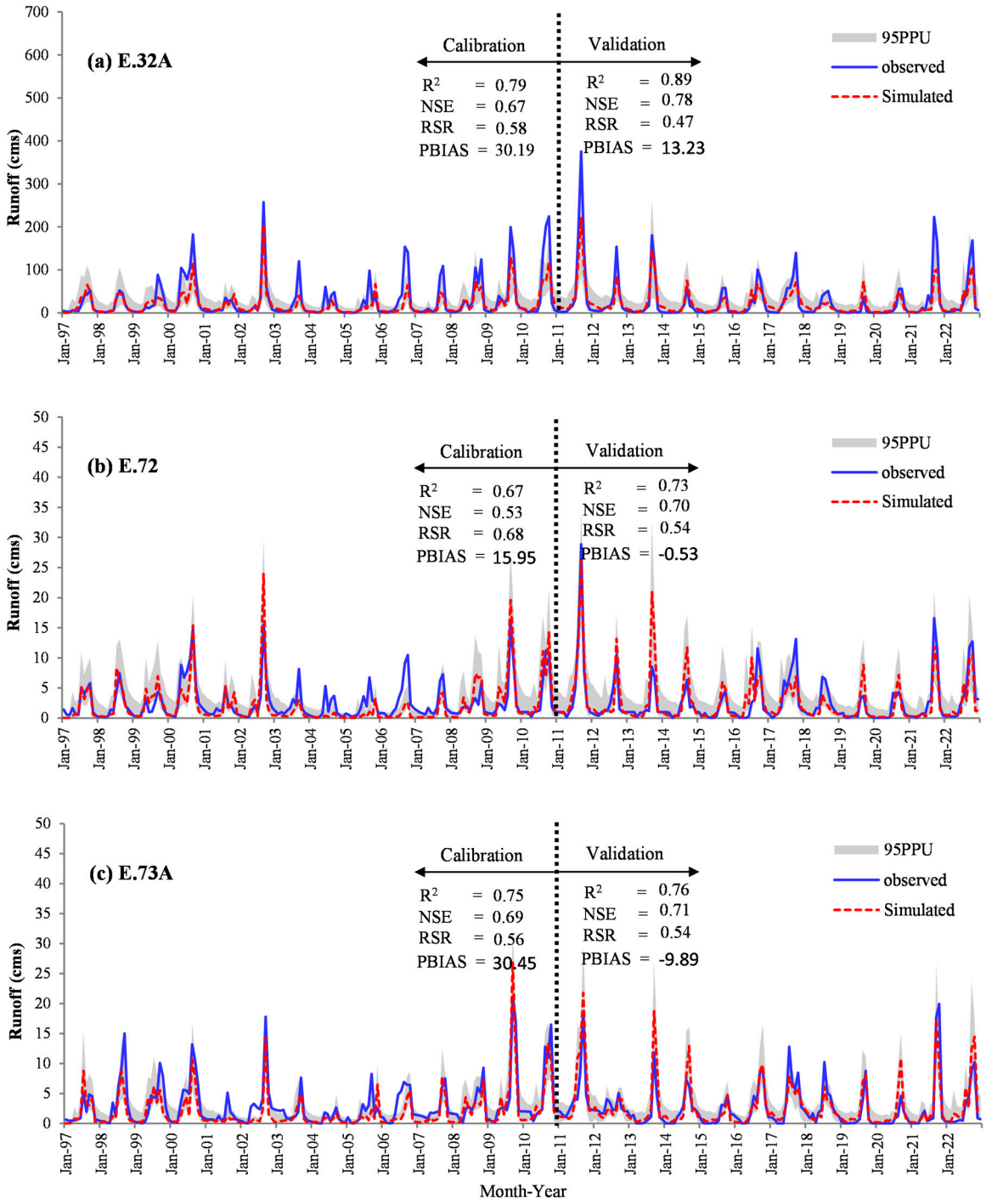

Figure 8. Calibration and validation of runoff analyzed by QSWAT; (a) Station E.32A, (b) Station E.72, (c) Station E.73A.

3.3. Efficiency Evaluation of QSWAT

3.3.1. Runoff components in depth unit

After the QSWAT was completely calibrated and validated, parameters were determined for 1997 – 2022 BL year runoff analysis. Runoff changes in depth unit were analyzed and the result was presented in spatial maps of subbasins properly by QSWAT for discussing changes based on basin boundary and elevation using watershed delineation [48]. For this study, therefore, there were 31 divided subbasins. This study was mainly to analyze the yield of runoff, so total runoff was determined as the whole amount of it (100%) [49] excluding the amount of water loss from

Preprints (www.preprints.org) | NOT PEER-REVIEWED | Posted: 5 September 2023 doi:10.20944/preprints202309.0338.v1

evapotranspiration. The previous study showed that evapotranspiration was 60% while remaining runoff was 40% [50]. Then runoff components were then analyzed and divided into 3 parts; surface runoff, interflow, and groundwater [51]. After considering monthly runoff components during BL year in terms of temporal change dimension, it was found that the surface runoff was the highest (71%) followed by interflow (21.6%) and groundwater (7.3%). The runoff was obviously seen in the rainy season (July - October), and the highest runoff occurred in August; surface runoff was 74.9 mm and interflow was 11.7 mm. After the rainy season ended, accumulated groundwater would be up to 2.7-3.4 mm during October – January as shown in Figure 9. The overall temporal changes in total runoff during base year depended on season in each region of Thailand as could be seen from its relation to monthly precipitation.

In considering spatial change dimension by the boundary of subbasins, the Subbasins 17, 18, 19, and 30 had the highest surface runoff (216 – 259 mm) as shown in Figure 10 (a) because they were the last stages of the current. However, it became lower in the midstream because it was agricultural land. The lowest surface runoff was found in the north because it was water source mostly covered with forest land, where it could store a small amount of surface runoff [52,53]. The midstream had a high chance of getting high in runoff because infiltration potential was lower [54]. As can be seen in Figure 10 (b), spatial change in groundwater was from moderate to high level in the north and midstream between 5 and 78 mm. The high level of runoff mostly occurred in the upper forest-covered and basin swamp that had high storage capacity [55,56]. Subbasin 3, 5, 8, 10, and 12 had the highest storage capacity (19-78 mm) while Subbasin 6, 7, 13, 14, 15, and 21 had the second highest storage capacity. There were 2 subbasins having very low level of groundwater including northwestern (Subbasins 1, 2, 9, 11, and 20) and southeastern (Subbasins 17, 18, 25, and 30). The cause of low groundwater was fast flow at the high slope area and the outlet point, which was consistent with the studies of Carroll et al. [56] and Nouayti et al. [57]. In case of interflow, most of the spatial changes could be seen at the outlet point of Subbasins 1, 10, 18, 19, and 25 as well as southwestern lowland, where distributary flowed across it (Subbasins 13 and 14), and some in the midstream including Subbasins 6 and 23 as presented in Figure 10 (c). Most of all, in considering the 3 runoff components represented by spatial condition of total runoff, it was found that the upper area having high slope and covered with forest was at low capacity to give total runoff. However, according to physical characteristic of the UCB, the total runoff from the upper area flowed down to the southern outlet. From this situation, its value was high between 205 – 389 mm as shown in Figure 10 (d).

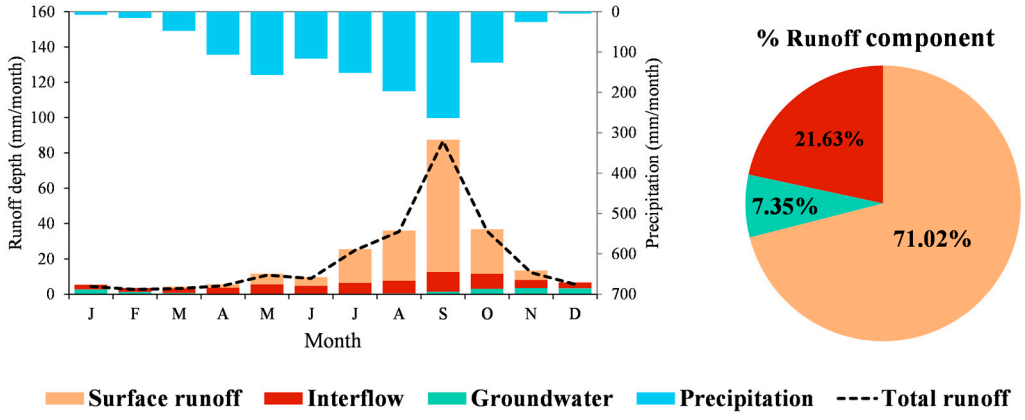

Figure 9. Temporal distribution of average monthly runoff components in depth unit for BL year.

Preprints (www.preprints.org) | NOT PEER-REVIEWED | Posted: 5 September 2023 doi:10.20944/preprints202309.0338.v1

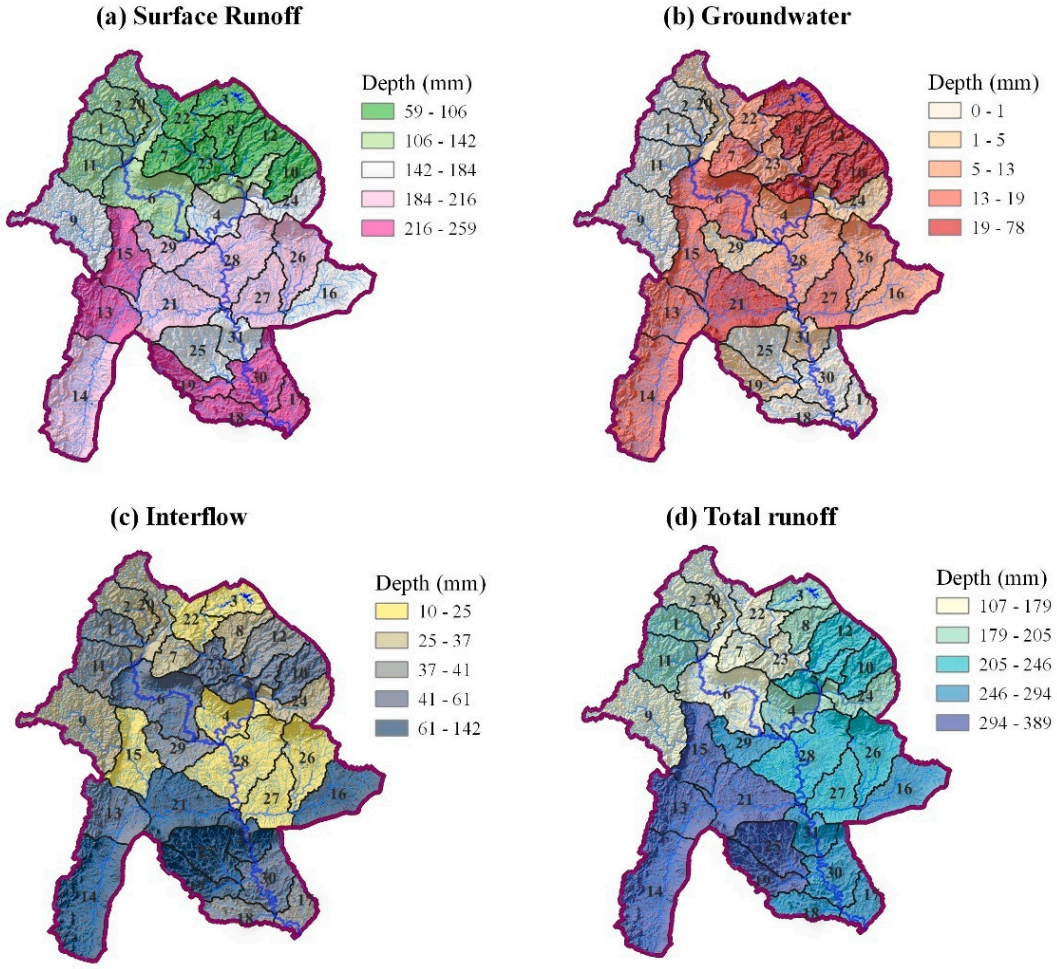

Figure 10. Spatial distribution of runoff components in depth unit during BL year; (a) surface runoff, (b) groundwater, (c) interflow, (d) total runoff.

3.3.2 Future runoff at the outlet point

The analysis result of future runoff at the outlet point (Subbasin 17, see Figure 10). When comparing the result between BL year and future year, average runoff during BL year was 835.3 MCM per year. In considering prediction scenarios and GCMs of SSP245 scenario, ACCESS-CM2 gave lowest different result from BL year (-1.8%) followed by MIROC6 (-4%). On the other hand, average runoff from MPI-ESM1-2-LR was 28.9% higher than BL year because of the increase in future precipitation. The result of runoff in SSP585 scenario showed higher variation than SSP245 scenario. It could be discussed that the average of ACCESS-CM2 was -15.4% lower than BL year because the 2041 - 2100 average runoff was -23.7% while the average of runoff obtained from MIROC6 was -5.3% different from BL year. The average runoff tended to be 21.8% lower during 2023 – 2060 but 11.2% higher during 2061 – 2100. On the other hand, rusults from the MPI-ESM1-2-LR was 11.3% - 175.6% higher than BL year, so its average was 106.6% different.

Nevertheless, when analyzing the overall average runoff at the outlet point of the UCB of 2 scenarios, the SSP245 scenario trend of increase was lower than SSP585 scenario. The SSP245 scenario showed its future long-term average of annual runoff of 899.2 MCM or 7.65% higher than BL year while SSP585 scenario showed its future long-term average of annual runoff of 1,057.8 MCM or 26.3% higher. The details of annual average evaluation of runoff by predictive time of each model are presented in Table 7. Moreover, long-term temporal changes in annual and monthly runoff during 2000 – 2100 were shown in Figure 11. It could be clearly seen that both SSP245 and SSP585 scenarios

Preprints (www.preprints.org) | NOT PEER-REVIEWED | Posted: 5 September 2023 doi:10.20944/preprints202309.0338.v1

were higher in future values. However, their trend lines were different because the line of SSP585 scenario was steeper than SSP245 scenario due to different increase rate of runoff.

This study results indicated the trend of overall changes in long-term runoff. The result of temporal changes in average monthly runoff at the outlet point analyzed by 3 types of GCM under 4 future predictive years during 2023 – 2100 based on SSP scenarios can be seen in Figure 12. The average future runoff during 2023 – 2060 (Figure 12 (a) – (b)) was close to BL year. By season, the dry season (March - June) showed slightly higher value than BL year (xx – yy %); however, it decrease in July and August. In rainy season (August), average runoff was higher and showed its maximum in October that both scenarios had close value between xx and yy MCM. Similarly, average 12-month runoff of both scenarios in the dry and rainy seasons during 2061 – 2100 showed obvious difference for SSP585 in October (maximum runoff); 350 MCM during 2061 – 2080 (xx% higher than BL year) and 400 MCM during 2081 – 2100 (xx% higher than BL year) (Figure 12 (c) – (d)). For SSP245 scenario, its maximum was close to BL year; however, the simulation result of future monthly runoff revealed that maximum runoff was in October, which was different from BL year in September.

According to a comparison between 4 periods of time and BL year, average monthly runoff of SSP585 during 2061 – 2100 would be higher than SSP245 and BL year especially maximum in October until the end of rainy season, and dry season from December to June next year. For this reason, it could be described that future average monthly runoff at the outlet point from QSWAT would be close to BL year during 2023 – 2060, and it would be higher during 2061 – 2100 especially SSP585 scenario as mentioned previously. In addition, the result also displayed periods of change in maximum runoff at least 1 month, and it kept getting high at the end of rainy season until dry season next year. This change would influence operational plan improvement of water resource management for flood control or water storage for drought period.

Table 7. Average annual runoff at outlet point of the UCB.

Periods/Years		Q_{avr} BL (MCM)	GCMs						Average	
			ACCESS-CM2		MIROC6		MPI-ESM1-2-LR			
			Q_{avr} (MCM)	BL Diff. (%)	Q_{avr} (MCM)	BL Diff. (%)	Q_{avr} (MCM)	BL Diff. (%)	Q_{avr} (MCM)	BL Diff. (%)
BL	2000 - 2022	835.3	-	-	-	-	-	-	-	-
SSP245	2023 - 2040	-	728.5	-12.8	826.6	-1.0	900.7	7.8	818.6	-2.0
	2041 - 2060	-	820.1	-1.8	636.2	-23.8	954.9	14.3	803.7	-3.8
	2061 - 2080	-	835.7	0.1	881.6	5.5	1,170.8	40.2	962.7	15.3
	2081 - 2100	-	896.4	7.3	856.2	2.5	1,283.1	53.6	1,011.9	21.1
SSP585	2023 - 2040	-	915.0	9.5	637.6	-23.7	930.0	11.3	827.5	-0.9
	2041 - 2060	-	615.7	-26.3	668.2	-20.0	1,383.3	65.6	889.1	6.4
	2061 - 2080	-	642.1	-23.1	922.1	10.4	2,288.3	174.0	1,284.2	53.7
	2081 - 2100	-	654.4	-21.7	735.0	12.0	2,301.6	175.6	1,230.3	47.3

Preprints (www.preprints.org) | NOT PEER-REVIEWED | Posted: 5 September 2023 doi:10.20944/preprints202309.0338.v1

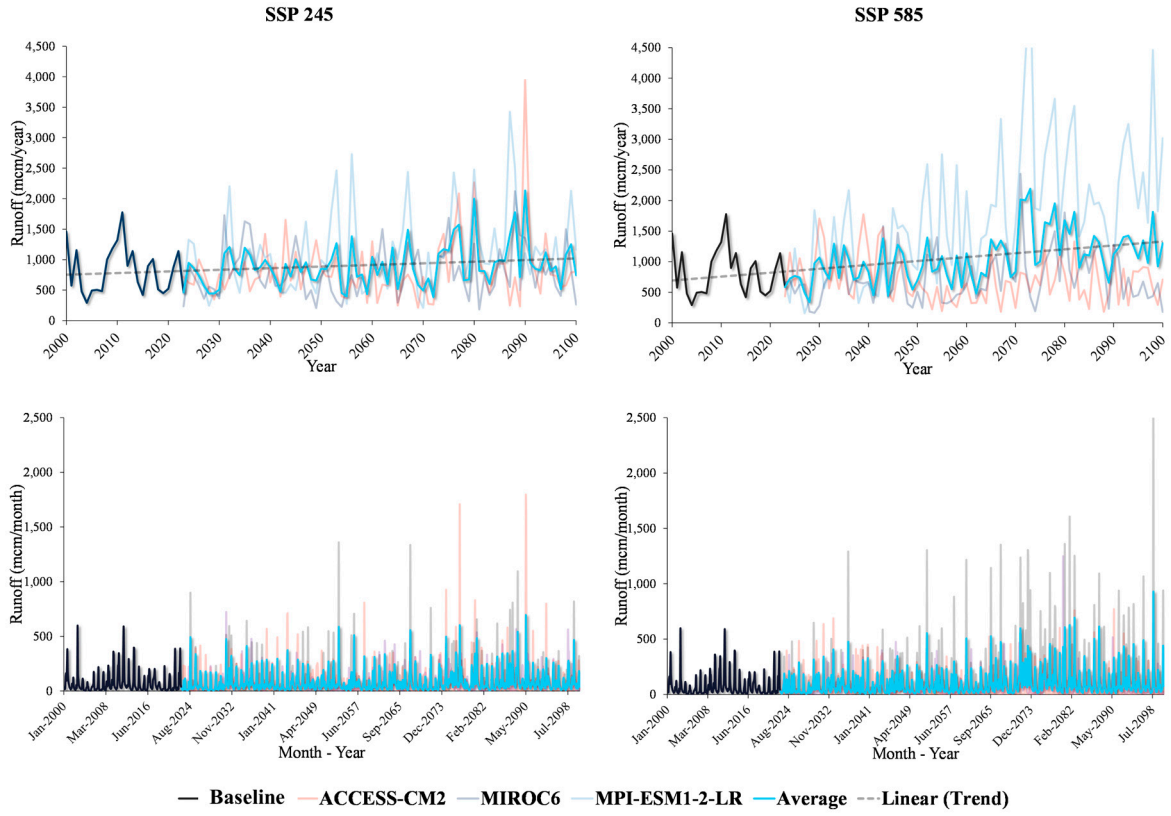

Figure 11. Long-term temporal changes in annual and monthly runoff during 2000-2100.

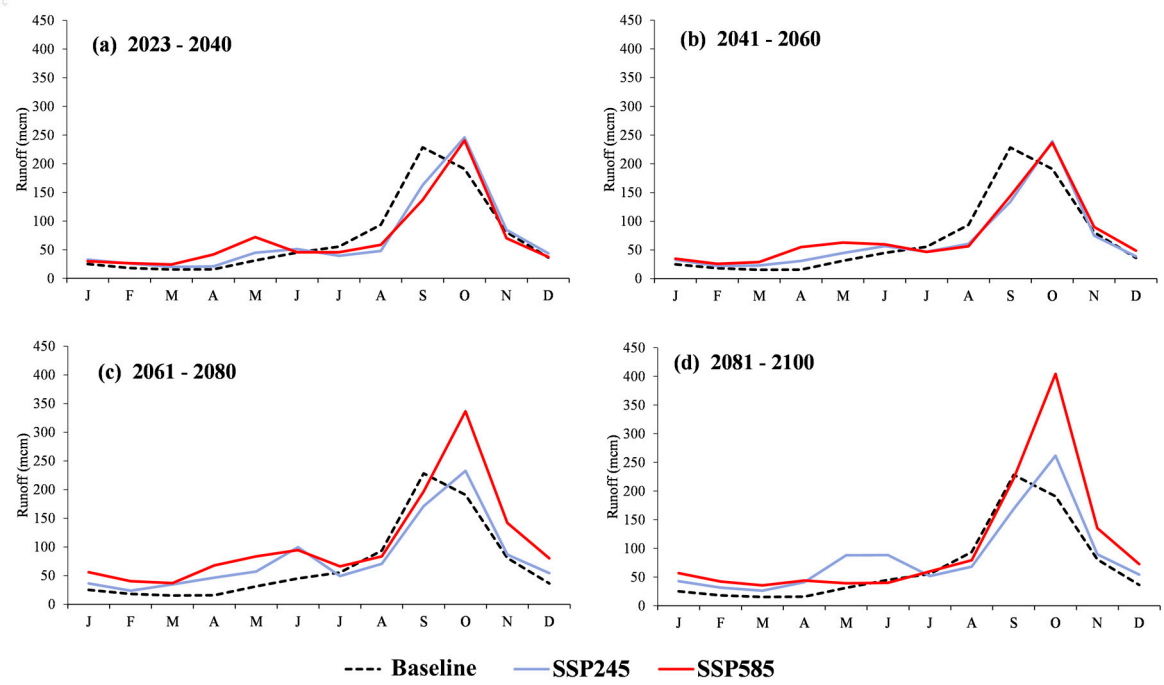

Figure 12. Comparison of average monthly runoff at outlet point of the UCB between 4 future predictive time periods and SSP scenarios; (a) 2023-2040, (b) 2041-2060, (c) 2061-2080, and (d) 2081-2100.

3.3.3. Future changes in runoff components

Changes in monthly runoff components in depth unit for SSP245 and SSP585 scenarios were analyzed under 4 periods of time during 2023 – 2100, and the result can be presented in Table 8.

Preprints (www.preprints.org) | NOT PEER-REVIEWED | Posted: 5 September 2023 doi:10.20944/preprints202309.0338.v1

According to the result, surface runoff with the highest ratio decreased between 9.6% – 12.7% for SSP245 scenario and 11.0% – 18.5% for SSP585 scenario, respectively. In the same way, interflow with second highest ratio decreased between 0.9% - 17.6% for SSP245 scenario but was 1.9% - 28.2% different for SSP585 scenario. On the other hand, changes in groundwater components tended to increase between 102.7% - 273% especially SSP585 scenario showing difference ratio during 2061 – 2100 that was 3 times higher than BL year.

Moreover, when considering monthly temporal changes (Figure 13) compared to BL year (Figure 9), total ratio of 3 part runoff components during August – October for SSP245 scenario was the highest although the total future runoff of 4 period of time (in the rainy season from July to August) would be lower than BL year. On the contrary, at the end of the rainy season (from October to June next year), total runoff would be higher than BL year. This change would be the same as one in SSP585 scenario during 2023 – 2060. Nevertheless, the ratio of all components would increase especially groundwater during and at the end of rainy season for both scenarios. Therefore, it was able to influence total monthly runoff and increase in accumulated runoff in the future.

Figure 14 presents the analysis result of spatial changes of future total runoff of each subbasin in depth unit compared to BL year (Figure 10 (d)) under 2 scenarios. This result reflected the consistency with temporal changes in runoff components as mentioned earlier. The changes of SSP245 and SSP585 scenarios during 2023 – 2060 would be similar. The northern or upstream area (Subbasins 1-3, 5-12, 20, and 22-23), where it was mostly covered with forest land, had higher changes in total runoff than BL year from 25.9% to 87.4%. The mid-stream area, where rice fields were replaced by sugarcane and cassava plantations, indicated its changes different because it not only increased but also decreased between 0.3% and -25.2%. However, the runoff in southern outlet points of Subbasins 17, 18, 25, and 30 was the lowest between 29.8% and 41.1%. During 2041 – 2060, furthermore, the subbasin with higher total runoff than BL year increased by 51.1% compared to previous time period and SSP245 scenario in the same time period. In considering both scenarios during 2061-2100, changes in most of the subbasins would be higher particularly SSP585 scenario, which 89.5% of the area showed an increase in changes between 3.3% and 197.1% from the upstream to the areas near the outlet point. However, the total runoff in the subbasins at the outlet point was lower than BL year between 14.1% and -36.3% especially SSP245 scenario in Subbasin 18.

In temporal change analysis applying watershed delineation by QSWAT to consider changes in total runoff by comparing between base year and long-term future year, over 90% of the area from the upstream to the outlet point tended to get higher in total runoff especially SSP585 scenario during 2061 – 2100. This increase in total runoff might be caused by increase in future precipitation in-between August and October, which could lead to the increases in groundwater and interflow consecutively.

Table 8. Comparative runoff component ration between BL and predictive years.

Runoff components	Ratio in BL period (%)	Scenario periods	Ratio in SSP245 and SSP585 (%)			
			SSP245	Diff.	SSP585	Diff.
Surface runoff	71.0	2023-2040	62.2	-12.4	63.2	-11.0
		2041-2060	63.8	-10.1	59.8	-15.8
		2061-2080	64.2	-9.6	56.9	-19.9
		2081-2100	62	-12.7	57.9	-18.5
Interflow	21.6	2023-2040	21.3	-1.4	21.2	-1.9
		2041-2060	21.4	-0.9	19.8	-8.3
		2061-2080	18.7	-13.4	15.5	-28.2
		2081-2100	17.8	-17.6	15.6	-27.8
Groundwater	7.4	2023-2040	16.5	123.0	15.6	110.8
		2041-2060	15	102.7	20.3	174.3

Preprints (www.preprints.org) | NOT PEER-REVIEWED | Posted: 5 September 2023 doi:10.20944/preprints202309.0338.v1

2061-2080	17.2	132.4	27.6	273.0
2081-2100	20.3	174.3	26.4	256.8

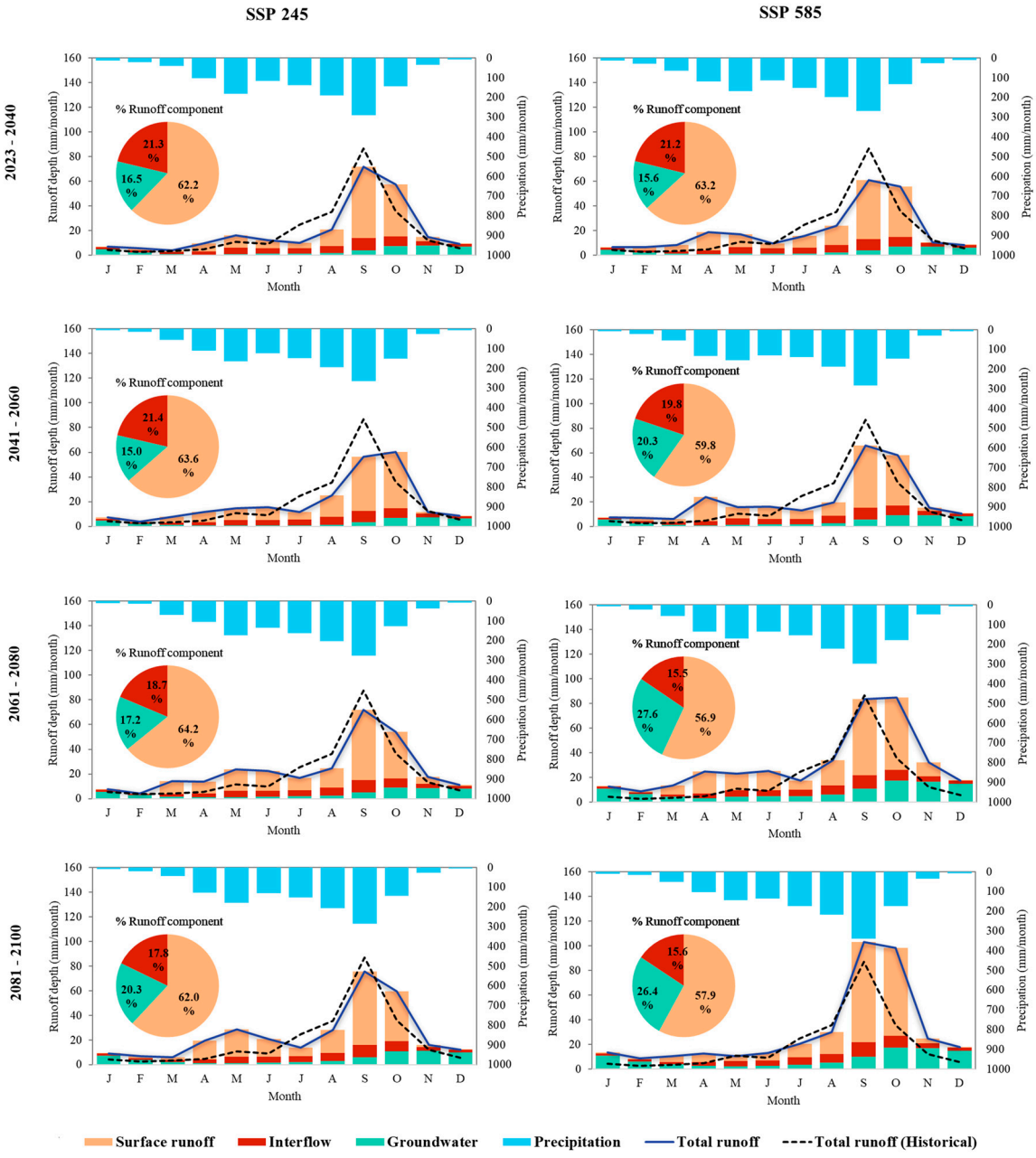

Figure 13. Comparison of average monthly runoff at outlet point during 2023 – 2100.

Preprints (www.preprints.org) | NOT PEER-REVIEWED | Posted: 5 September 2023 doi:10.20944/preprints202309.0338.v1

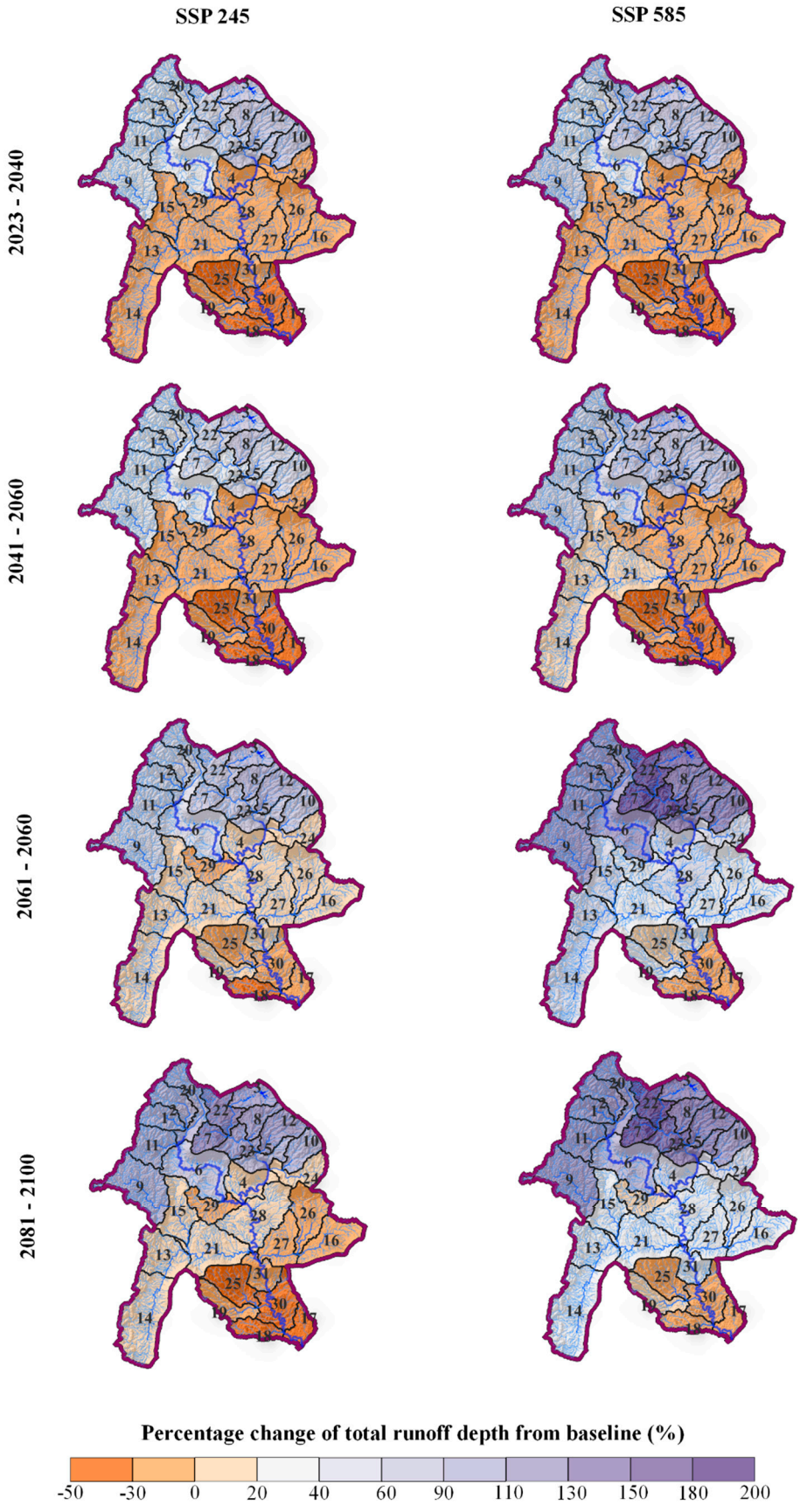

Figure 14. Spatial changes of total runoff in depth unit by scenarios and future times. .

 doi:10.20944/preprints202309.0338.v1

4. Conclusion

This study tried to understand the uncertainty of climate and land use changes impact on runoff and its components. The Upper Chi Basin (UCB) was selected for the study because it is the main headwaters of the Chi River in Northeastern Thailand. The basin has encountered water resource problems in dry and flood seasons as well as changes in land use for agricultural activities and habitation. These problems affect the runoff and its components that can lead to future variation, which is the main focus of this study. According to literature review, research design, and selected optimal research tools, the results can be concluded as follows;

First of all, climate change was analyzed using 3 types of GCM-CMIP6 models including ACCESS-CM2, MIROC6, and MPI-ESM1-2-LR, under SSP245 and SSP585 scenarios during 2023-2100. The result revealed that the average monthly precipitation of SSP585 was higher than BL year while the average of SSP245 was close to BL year. According to annual total precipitation of SSP585, it tended to increase and have higher average than SSP245. The analysis result of future changes in maximum and minimum temperature showed that the monthly average of 3 GCMs in SSP245 was close to BL year and tended to increase in the future. However, the future of SSP585 that was far from BL year showed high trend in maximum and minimum temperatures. Based on the analysis result of the annual average of future long-term temporal changes, SSP585 tended to get higher than SSP245. The effect from SSP585 reflected higher variation especially maximum temperature.

Secondly, future changes in land use was analyzed by Land Change Modeler (LCM) using historical land use maps under 2 periods of time, which were 2015 and 2019, as primary data for analysis. The analysis result in BL year revealed that forest land was most appeared and it tended to decrease, followed by rice fields and cassava plantations. In spatial distribution, LCM demonstrated the future situation of forest land, which would be replaced by sugarcane plantations especially mid-stream and southern part of basin. In case of comparing the future increased area with BL year, sugarcane showed the highest trend followed by mixed field crop of rubber tree and mixed orchard. The spatial expansion was found that increased sugarcane land use would replace forest and rice fields around mid-stream and southern of the UCB.

Finally, changes in future runoff and its components were analyzed by QSWAT. The result indicated that QSWAT had potential to analyze runoff and hydrological components properly as can be seen from acceptable statistical indices including R^2, NSE, RSR, and PBIAS. This could lead to long-term temporal and spatial changes by depth of 31 subbasins. The analysis result of runoff at the outlet point of the UCB comparing between BL year and future condition, the average runoff of SSP245 was slightly lower while SSP585 tended to be higher. Additionally, it can be described that runoff in October was the highest which was different from September of existing BL year, and SSP585 tended to have higher than SSP245.

When considering the variation of total runoff and monthly runoff components in depth unit from 2 future scenarios, surface runoff with highest ratio became lower the same as interflow. On the other hand, groundwater tended to become higher especially at the end of rainy season, which might affect an increase in future annual and monthly total runoff. Based on the analysis result of spatial changes in future total runoff compared to BL year, the headwater area in the north part illustrated higher change in total runoff. In mid-stream area, where rice fields were replaced by sugarcane and cassava plantations, total runoff variation got both higher and lower while it was lower at the outlet point. However, SSP585 demonstrated that most of the basin area had higher total runoff. In case of long-term changes, over 90% from the up-stream area to the outlet point tended to be higher in total runoff due to an increase in future precipitation that could affect both groundwater and interflow respectively.

Above all, understanding the effects of climate and land use changes on runoff and components in the UCB applying historical and statistical data to efficient mathematical models as well as methodology used in this study can help receive reliable long-term temporal and spatial results to understand changes in meteorological dimension and LULC. Both temporal and spatial changes became important factors influencing changes in hydrological system especially runoff in the basin. The result of this study can be important data to understanding future and current changes in

hydrological system and to decision making. Moreover, it can be useful for stakeholders who are responsible for water management in the UCB to design a plan to develop water management system and handle any effects on different dimensions properly and sustainably under changes happening in the future.

Author Contributions: Conceptualization, R.H., A.K. and H.P.; methodology, R.H., S.K., A.K., J.K, K.B., K.S., S.M., S.S and H.P; software, R.H., S.K., J.K, K.B., S.M., S.S and H.P.; validation, R.H., S.K., J.K, K.B., S.M., S.S and H.P.; formal analysis, R.H. and H.P.; investigation, R.H. and H.P.; resources, R.H. and H.P.; data curation, R.H. and H.P.; writing—original draft preparation, H.P. and R.H.; writing—review and editing, H.P., R.H. and A.K.; visualization, H.P.; supervision, A.K.; project administration, A.K. and K.S.; funding acquisition, R.H. and A.K. All authors have read and agreed to the published version of the manuscript.

Funding: This research was funded by Thailand Science Research and Innovation (TSRI) in fiscal year 2022 supported the research project named "The impact of climate and land use changes uncertainty on water balance and water yield management in Chi River Basin", under the administration by the Faculty of Engineering, Mahasarakham University, Thailand.

Acknowledgments: We would like to extend our gratitude to the Royal Irrigation Office 6, Khon Kaen for giving us hydrological data, the Land Development Office 5 for supporting soil type and land use data, and the Upper Northeastern Meteorological Center for providing meteorological data. Our thanks and appreciations also go to scholars and specialists from different educational institutes and organizations related to water resource management for giving us suggestions on hydro-meteorological analysis as well as applying mathematical models that are helpful to us for research discussion.

Conflicts of Interest: The authors declare no conflict of interest.

References

1. Bouabdelli, S.; Meddi, M.; Zeroual, A.; Alkama, R. Hydrological Drought Risk Recurrence Under Climate Change in the Karst Area of Northwestern Algeria. *J. Water Clim. Chang*. **2020**, *11 (S1)*, 164–188.
2. Tan, M.L.; Liang, J.; Samat, N.; Chan, N.W.; Haywood, J.M.; Hodges, K. Hydrological Extremes and Responses to Climate Change in the Kelantan River Basin, Malaysia, Based on the CMIP6 HighResMIP Experiments. *Water*. **2021**, 13, *1472*. https://doi.org/10.3390/w13111472.
3. Bal, M.; Dandpat, A.K.; Naik, B. Hydrological Modeling with Respect to Impact of Land-use and Land-cover Change on the Runoff Dynamics in Budhabalanga River Basing using ArcGIS and SWAT Model. *Remote Sens. Appl.: Soc. Environ*. **2021**, *23*, August 2021, *100527*. https://doi.org/10.1016/j.rsase.2021.100527.
4. Liu, S.; Li, X.; Chen, D.; Duan, Y.; Ji, H.; Zhang, L.; Chai, Q.; Hu, X. Understanding Land use/Land cover Dynamics and Impacts of Human Activities in the Mekong Delta Over the Last 40 Years. *Glob. Ecol. Conserv*. **2020**, 22, June 2020, *e00991*. https://doi.org/10.1016/j.gecco.2020.e00991.
5. Arowolo, A.O.; Deng, X. Land use/land cover change and statistical modelling of cultivated land change drivers in Nigeria. *Reg. Environ. Change*. **2018**, 18, 247–259. https://doi.org/10.1007/s10113-017-1186-5.
6. Wang, Z.; Han, Q.; de Vries, B. Land Use/Land Cover and Accessibility: Implications of the Correlations for Land Use and Transport Planning. *Appl. Spatial Analysis.* **2019**, 12, 923–940. https://doi.org/10.1007/s12061-018-9278-2.
7. Bao, Q.; Ding, J.; Han, L.; Li, J. Ge, X. Predicting Land Change Trends and Water Consumption in Typical Arid Regions using Multi-models and Multiple Perspectives. *Ecol. Indic*. **2022**, 141, August 2022, *109110*. https://doi.org/10.1016/j.ecolind.2022.109110.
8. Kaushal, S.S.; Gold, A.J.; Mayer, P.M. Land Use, Climate, and Water Resources—Global Stages of Interaction. *Water*. **2017**, *9*, 815. https://doi.org/10.3390/w9100815.
9. Haq, M.; Iqbal, M.J.; Alam, K.; Huang, Z.; Blaschke, T.; Qureshi, S.; Muhammad, S. Assessment of Runoff Components of River Flow in the Karakoram Mountains, Pakistan, during 1995–2010. *Remote Sens*. **2023**, 15, *399*. https://doi.org/10.3390/rs15020399.
10. Schwab, M. P.; Klaus, J.; Pfister, L.; Weiler, M. How Runoff Components Affect the Export of DOC and Nitrate: a Long-term and High-frequency Analysis. *Hydrol. Earth Syst. Sci. Discuss.* **2017**, https://doi.org/10.5194/hess-2017-416.
11. Xuan, W.; Fu, Q.; Qin, G.; Zhu, C.; Pan, S.; Xu, Y.-P. Hydrological Simulation and Runoff Component Analysis over a Cold Mountainous River Basin in Southwest China. *Water.* **2018**, 10, 1705. https://doi.org/10.3390/w10111705.
12. Calderon, H.; Uhlenbrook, S. Characterizing the Climatic Water Balance Dynamics and Different Runoff Components in a Poorly Gauged Tropical Forested Catchment, Nicaragua. *Hydrol. Sci. J*. **2016**, *61(14)*, 2465–2480. http://dx.doi.org/10.1080/02626667.2014.964244.

13. Hyandye, C.B.; Worqul, A.; Martz, L.W.; Muzuka, A.N.N. The Impact of Future Climate and Land use/cover Change on Water Resources in the Ndembera Watershed and Their Mitigation and Adaptation Strategies. *Environ Syst Res.* **2018**, *7*. https://doi.org/10.1186/s40068-018-0110-4.
14. Mahmoud, S.H.; Gan, T.Y. Urbanization and Climate Change Implications in Flood Risk Management: Developing an Efficient Decision Support System for Flood Susceptibility Mapping. *Sci. Total Environ.* **2018**, *636*, 152-167. https://doi.org/10.1016/j.scitotenv.2018.04.282.
15. Janjić, J.; Tadić, L. Fields of Application of SWAT Hydrological Model—A Review. *Earth,* **2023**, *4*, 331-344. https://doi.org/10.3390/earth4020018.
16. Kalogeropoulos, K.; Stathopoulos, N.; Psarogiannis, A.; Pissias, E.; Louka, P.; Petropoulos, G.P.; Chalkias, C. An Integrated GIS-Hydro Modeling Methodology for Surface Runoff Exploitation via Small-Scale Reservoirs. *Water*, **2020**, *12*, 3182. https://doi.org/10.3390/w12113182.
17. Dile, Y.T.; Daggupati, P.; George, C.; Srinivasan, R.; Arnold, J. Introducing a New Open Source GIS User Interface for the SWAT Model. *Environ. Model Softw.* **2016**, *85*, 129-138. https://doi.org/10.1016/j.envsoft.2016.08.004.
18. Nielsen, A.; Bolding, K.; Hu, F.; Trolle, D. An Open Source QGIS-based Workflow for Model Application and Experimentation with Aquatic Ecosystems. *Environ. Model Softw.* **2017,** 358-364. https://doi.org/10.1016/j.envsoft.2017.06.032.
19. Reddy, N.N.; Reddy, K.V.; Vani, J.S.L.S.; Daggupati, P.; Srinivasan, R. Climate Change Impact Analysis on Watershed using QSWAT. *Spat. Inf. Res.* **2018,** *26*, 253–259. https://doi.org/10.1007/s41324-017-0159-6.
20. Munoth, P.; Goyal, R. Hydromorphological Analysis of Upper Tapi River Sub-basin, India, using QSWAT Model. Model. *Earth Syst. Environ.* **2020**, *6*, 2111–2127. https://doi.org/10.1007/s40808-020-00821-x.
21. Tanksali, A.; Soraganvi, V.S. Assessment of Impacts of Land Use/Land Cover Changes Upstream of a Dam in a Semi-arid Watershed using QSWAT. *Model. Earth Syst. Environ.* **2021**, *7*, 2391–2406. https://doi.org/10.1007/s40808-020-00978-5.
22. Petrie, R.; Denvil, S.; Ames, S.; Levavasseur, G.; Fiore, S.; Allen, C.; Antonio, F.; Berger, K.; Bretonnière, P.-A., Cinquini, L., Dart, E., Dwarakanath, P., Druken, K., Evans, B., Franchistéguy, L.; Gardoll, S.; Gerbier, E.; Greenslade, M.; Hassell, D.; Iwi, A.; Juckes, M.; Kindermann, S.; Lacinski, L.; Mirto, M.; Nasser, A. B.; Nassisi, P.; Nienhouse, E.; Nikonov, S.; Nuzzo, A.; Richards, C.; Ridzwan, S.; Rixen, M.; Serradell, K.; Snow, K.; Stephens, A.; Stockhause, M.; Vahlenkamp, H.; Wagner, R. Coordinating an Operational Data Distribution Network for CMIP6 Data, *Geosci. Model Dev.* **2021**, *14*, 629–644, https://doi.org/10.5194/gmd-14-629-2021.
23. Tariq, A.; Yan, J.; Mumtaz, F. Land change modeler and CA-Markov chain analysis for land use land cover change using satellite data of Peshawar, Pakistan. *Phys. Chem. Earth.* **2022**, 128, 103286. https://doi.org/10.1016/j.pce.2022.103286.
24. Motlagh, S.K.; Sadoddin, A.; Haghnegahdar, A.; Razavi, S.; Salmanmahiny, A.; Ghorbani, K. Analysis and Prediction of Land Cover Changes using the Land Change Modeler (LCM) in a Semiarid River Basin, Iran. *Land Degrad Dev.* **2021**, 32(10), 3092-3105. https://doi.org/10.1002/ldr.3969.
25. Akdeniz, H.B.; Sag, N.S.; Inam, S. Analysis of Land Use/Land Cover Changes and Prediction of Future Changes with Land Change Modeler: Case of Belek, Turkey. Environ. Monit. Assess. **2023**, *195*, 135. https://doi.org/10.1007/s10661-022-10746-w.
26. Dix, M.; Bi, D.; Dobrohotoff, P.; Fiedler, R.; Harman, I.; Law, R.; Yang, R. CSIRO-ARCCSS ACCESS-CM2 model output prepared for CMIP6 CMIP historical. *Earth System Grid Federation*. 2019, https://doi. org/10.22033/ESGF/CMIP6, 4271.
27. Shiogama, H.; Abe, M.; Tatebe, H. MIROC MIROC6 model output prepared for CMIP6 ScenarioMIP, **2019**, *800*. https://doi. org/10.22033/ESGF.
28. Wieners, K. H.; Giorgetta, M.; Jungclaus, J.; Reick, C.; Esch, M.; Bittner, M.; Roeckner, E. MPI-M MPI-ESM1. 2-LR model output prepared for CMIP6 ScenarioMIP ssp245. Version YYYYMMDD. **2019**, Earth System Grid Federation.
29. Brighenti, T.M.; Gassman, P.W.; Gutowski, W.J., Jr.; Thompson, J.R. Assessing the Influence of a Bias Correction Method on Future Climate Scenarios Using SWAT as an Impact Model Indicator. *Water*, **2023**, 15, 750. https://doi.org/10.3390/w15040750.
30. Tadese, M.T.; Kumar, L.; Koech, R. Climate change projections in the Awash River Basin of Ethiopia using Global and Regional Climate Models. *Int. J. Climatol*. **2019**, *40(8)*, 3649-3666. https://doi.org/10.1002/joc.6418.
31. Senganatham, N.; Souvannasouk, V.; Moonphoxay, H.; Fongsamoth, S. Optimal Long-term Rainfall Trends Prediction under Climate Change Scenarios in Small Basin: Case study Sedon Basin, Lao PDR. *Maejo Int. J. Energ. Environ. Comm.* **2021**, *3(3)*, 70–73.
32. Yeboah, K.A.; Akpoti, K.; Kabo-bah, A.T.; Ofosu, E.A.; Siabi, E.K.; Mortey, E.M.; Okyereh, S.A. Assessing Climate Change Projections in the Volta Basin using the CORDEX-Africa Climate Simulations and Statistical Bias-correction. *Environ. Chall*. **2022,** *6*, 100439. https://doi.org/10.1016/j.envc.2021.100439.
33. Yang, X.; Zheng, X.Q.; Chen, R. A Land Use Change Model: Integrating Landscape Pattern Indexes and Markov-CA. **2014**, 283, 1-7. https://doi.org/10.1016/j.ecolmodel.2014.03.011.

34. Kumar, V.; Agrawal, S. A Multi-layer Perceptron–Markov Chain Based LULC Change Analysis and Prediction using Remote Sensing Data in Prayagraj District, India. *Environ. Monit. Assess.* **2023**, *195*, 619. https://doi.org/10.1007/s10661-023-11205-w.
35. Dashavant, P. B.; Dandu, M.M. Estimation of Water Balance Components of Patapur Micro Watershed in the Tungabhadra River Basin Using QSWAT Model in QGIS Environment. *Int. J. Environ. Clim.* **2022**, *12(12)*, 1013-1028.
36. Thavhana, M.P.; Savage, M.J.; Moeletsi, M.E. SWAT Model Uncertainty Analysis, Calibration and Validation for Runoff Simulation in the Luvuvhu River Catchment, South Africa. *Phys. Chem. Earth.* **2018**, *105*, 115-124. https://doi.org/10.1016/j.pce.2018.03.012.
37. Chawanda, C. J.; George, C.; Thiery, W.; Van Griensven, A.; Tech, J.; Arnold, J.; Srinivasan, R. (2020). User-friendly workflows for catchment modelling: Towards reproducible SWAT+ model studies. *Environ. Model. Softw.* **2020,** *134*, 104812.
38. Koua, T. J. J.; Dhanesh, Y.; Jeong, J.; Srinivasan, R.; Anoh, K. A. Implementation of the Semi-distributed SWAT (Soil and Water Assessment Tool) Model Capacity in the Lobo Watershed at Nibéhibé (Center-West of Côte d'Ivoire). *J. Geosci. Environ. Prot.* **2021**, *9(8)*, 21-38.
39. Munoth, P.; Goyal, R. Effects of Area Threshold Values and Stream Burn-in Process on Runoff and Sediment Yield using QSWAT model, *ISH J. Hydraul. Eng.* **2022,** *28*, 40-48, https://doi.org/10.1080/09715010.2019.1670107.
40. Rossetto, R.; Cisotto, A.; Dalla Libera, N.; Braidot, A.; Sebastiani, L.; Ercoli, L.; Borsi, I. ORGANICS: A QGIS Plugin for Simulating One-Dimensional Transport of Dissolved Substances in Surface Water. *Water*, **2022**, 14, 2850. https://doi.org/10.3390/w14182850
41. Aytaç, E. Unsupervised Learning Approach in Defining the Similarity of Catchments: Hydrological Response Unit Based K-means Clustering, a Demonstration on Western Black Sea Region of Turkey. *Int. Soil Water Conserv. Res.* 2020, *8(3)*, 321-331. https://doi.org/10.1016/j.iswcr.2020.05.002.
42. Tuppad, P.; Douglas-Mankin, K. R.; Lee, T.; Srinivasan, R.; Arnold, J. G. Soil and Water Assessment Tool (SWAT) Hydrologic/Water Quality Model: Extended Capability and Wider Adoption. *Trans ASABE*, **2011**, *54(5)*, 1677-1684.
43. Sao, D.; Kato, T.; Tu, L.H.; Thouk, P.; Fitriyah, A.; Oeurng, C. Evaluation of Different Objective Functions Used in the SUFI-2 Calibration Process of SWAT-CUP on Water Balance Analysis: A Case Study of the Pursat River Basin, Cambodia. *Water*, **2020**, 12, 2901. https://doi.org/10.3390/w12102901.
44. Malik, M. A.; Dar, A. Q.; Jain, M. K. Modelling Streamflow using the SWAT Model and Multi-site Calibration Utilizing SUFI-2 of SWAT-CUP Model for High Altitude Catchments, NW Himalaya's. *Model. Earth Syst. Environ.* **2022**, 8, 1203–1213. https://doi.org/10.1007/s40808-021-01145-0.
45. Tejaswini, V., & Sathian, K. K. Calibration and Validation of SWAT Model for Kunthipuzha Basin using SUFI-2 Algorithm. *Int. J. Curr. Microbiol. Appl. Sci.* **2018**, *7(1)*, 2162-72.
46. Abbaspour, K. C.; Vejdani, M.; Haghighat, S.; Yang, J. SWAT-CUP Calibration and Uncertainty Programs for SWAT. In the Proceeding of MODSIM 2007 International Congress on Modelling and Simulation, Modelling and Simulation Society of Australia and New Zealand. **2007**, 1596-1602. Dübendorf, Switzerland: Swiss Federal Institute of Aquatic Science and Technology.
47. Zhang, S.; Li, Z.; Lin, X.; Zhang, C. Assessment of Climate Change and Associated Vegetation Cover Change on Watershed-Scale Runoff and Sediment Yield. *Water*, **2019**, 11, 1373. https://doi.org/10.3390/w11071373.
48. Chen, M.; Cui, Y.; Gassman, P.W.; Srinivasan, R. Effect of Watershed Delineation and Climate Datasets Density on Runoff Predictions for the Upper Mississippi River Basin Using SWAT within HAWQS. *Water*, **2021**, *13*, 422. https://doi.org/10.3390/w13040422.
49. Nazari-Sharabian, M.; Taheriyoun, M.; Karakouzian, M. Sensitivity Analysis of the DEM Resolution and Effective Parameters of Runoff Yield in the SWAT model: a Case Study. *J. Water Supply: Res. Technol. - AQUA*. **2020**, *69(1)*, 39–54. http://doi: https://doi.org/10.2166/aqua.2019.044.
50. Prasanchum, H.; Kangrang, A.; Hormwichian, R. Change in Inflow and Hydrologic Response due to Proactive Agriculture Land Use Policy in Northeast of Thailand. *Int. Rev. Civ. Eng*, **2020**, *11*, 141-151.
51. Chen, Y.; Wang, L.; Shi, X.; Zeng, C.; Wang, Y.; Wang, G.; Qiangba, C.; Yue, C.; Sun, Z.; Renzeng, O.; et al. Impact of Climate Change on the Hydrological Regimes of the Midstream Section of the Yarlung Tsangpo River Basin Based on SWAT Model. *Water*, **2023**, *15*, 685. https://doi.org/10.3390/w15040685.
52. Lotfalian, M.; Babadi, T. Y.; Akbari, H. Impacts of Soil Stabilization Treatments on Reducing Soil Loss and Runoff in Cutslope of Forest Roads in Hyrcanian Rorests. *Catena*, **2019**, *172*, 158-162.
53. Wang, D.; Yu, X.; Jia, G.; Wang, H. Sensitivity Analysis of Runoff to Climate Variability and Land-Use Changes in the Haihe Basin Mountainous Area of North China. *Agric. Ecosyst. Environ.* **2019**, *269*, 193-203.
54. Bombino, G.; Denisi, P.; Gómez, J.A.; Zema, D.A. Water Infiltration and Surface Runoff in Steep Clayey Soils of Olive Groves under Different Management Practices. *Water*, **2019**, 11, 240. https://doi.org/10.3390/w11020240.

55. Filoso, S.; Bezerra, M.O.; Weiss, K.C.; Palmer, M.A. Impacts of Forest Restoration on Water Yield: A Systematic Review. *PloS one*, **2017**, *12(8)*, e0183210.
56. Carroll, R. W.; Deems, J. S.; Niswonger, R.; Schumer, R.; Williams, K. H. The Importance of Interflow to Groundwater Recharge in a Snowmelt-Dominated Headwater Basin. *Geophys. Res. Lett.* **2019**, 46(11), 5899-5908. https://doi.org/10.1029/2019GL082447.
57. Nouayti, A.; Khattach, D.; Hilali, M.; Nouayti, N. Mapping Potential Areas for Groundwater Storage in the High Guir Basin (Morocco): Contribution of Remote Sensing and Geographic Information System. *J. Groundw. Sci. Eng.* **2019**, *7(4)*, 309-322. https://doi.org/10.19637/j.cnki.2305-7068.2019.04.002.